Available online at www.sciencedirect.com
ScienceDirect
Journal of Power Sources 179 (2008) 417–423
JOURNAL OF POWER SOURCES
www.elsevier.com/locate/jpowsour

Optimal battery/ultracapacitor storage combination

William Henson *

University of Massachusetts, Mechanical and Industrial Engineering Department, Renewable Energy Research Laboratory, United States

Received 12 October 2007; received in revised form 17 December 2007; accepted 18 December 2007
Available online 4 January 2008

Abstract

A simple, global model for the optimal combination of ultracapacitor and battery for electrical energy storage is developed. The goal for this hybrid storage technology is to reduce the system life-cycle cost by making use of an ultracapacitor's claimed long cycling-life in order to supplement relatively cheap, but cycle-limited battery storage. The model is built up of two independent sub-models that allow flexibility in the relative proportion of system energy storage. An analysis performed in this paper indicates that ultracapacitor/battery storage systems may be cost effective for high-cycle applications.

Keywords: Short-term storage; Optimal combination; Power smoothing

1. Introduction

Renewable energy systems that make use of fluctuating prime-movers (e.g. wind power) produce power that also fluctuates on several time-scales. For a wind power system, time-scale fluctuations range from the slowest, such as fluctuations over the course of several years (e.g. El Nino effects), to seasonal variations (e.g. in some areas the wind blows stronger and more consistently in the Winter), to short time-scale fluctuations on the order of seconds up to an hour. Though the grid-connected load also varies; in many cases, it is desirable to smooth out these generation fluctuations to some degree.

There are three main techniques that can be applied in smoothing out wind power fluctuations (1) Aggregation of spatial diversity both within wind-farms and between wind-farms (or single installations) (2) Aggregation of generation diversity that uses other means of generation that may possess different fluctuation characteristics or that may be throttled and (3) Storage of surplus energy in order to release the surplus during times of power generation deficit. Different storage technologies have differing characteristics that make the particular technology more or less suitable for reducing the variability over particular time-scales and for particular scales of energy amounts. For instance, pumped hydro storage is particularly well-suited for reducing variability in the hours-to-days time-frame for very large amounts of energy, while batteries are more well suited for the second to hour time-frame for much more modest amounts of energy. It may be beneficial to combine storage technologies into systems that allow each specific technology to concentrate on its "best fit" of time-scale and energy-scale, thereby creating a storage system that can deal more effectively with variations from power sources. Besides power source smoothing, a well-matched storage system could also be useful in a variety of other applications (e.g. power smoothing for variable loads).

As one example of power variability, take for instance one source (namely tower shadow) in an example state-of-the-art electricity producing wind turbine with a nameplate rating of 2 mW and an overall design lifetime of approximately 20 years. The turbine rotor will rotate at approximately 15 rpm at rated speed. As the three blades pass in front of the tower, they will pass through a small area of reduced will speed directly in front of the tower. This tower shadow effect reduces the wind turbine output by up to approximately 1% and lasts for up to approximately 5° of rotation. Assuming a square wave for the power pulse, the net effect of this tower shadowing causes a 0.75 Hz 56 ms duration 20 kW power dip for this example turbine. As the mean wind speed fluctuates, so too will the turbine rpm, produced power, and hence the duration, frequency, and magnitude of the power dip; however, if the turbine is placed in a favorable wind regime it will be operating at rated speed for much of the time. As a conservative estimate, let the wind turbine operate at rated speed

* Corresponding author. Tel.: +1 413 545 0540; fax: +1 413 577 1301.
E-mail address: henson_eng@yahoo.com.
URL: http://rerl.org.

0378-7753/$ – see front matter © 2008 Elsevier B.V. All rights reserved.
doi:10.1016/j.jpowsour.2007.12.083

Nomenclature

$a1, a2, a3$	coefficients for exponential fit
BBS	baseline battery system
C_F	cycles to failure for battery
DOD	depth of discharge
RMSE	root mean squared error
$2 \times (0.1U + 0.9$ BS)	combination system with 2 times energy capacity of BBS, utilizing 10% Ucap
Ucap	ultracapacitor

for 10% of the year (i.e. a 10% cycling duty cycle), this translates into roughly 2.4 million cycles per year of this example power dip.

Sources of power variability in a wind turbine are not limited only to tower shadow; wind field non-uniformity across the rotor disk (i.e. turbulence and shear) and wind field non-uniformity over time (i.e. wind gusts), as well as switching operations within the electrical (and sometimes mechanical) components and actuator lag in the turbine all contribute to short-term power fluctuations. Given the wind turbine 20 year design lifetime, a very large number of cycles (in excess of 10^6) could certainly be achieved by fluctuations with cycling frequencies on the order of 0.016 Hz. This cycling with a period of about 1 min falls in a relatively high-energy portion of the wind spectrum [1–3], and so a high cycling duty cycle is likely. A smoothing system could be envisaged that would reduce the magnitude of power fluctuations resulting in a more desirable constant power output on the short-term time-scale. A sophisticated design will take all sources of variability into account. In other words, a short-term storage system should be designed to balance the desires to smooth power over a range of fluctuations: from those induced by tower shadow (low energy, high cycling frequency) to those induced by wind gusts (moderate energy, low cycling frequency), perhaps even up to those caused by slightly longer-term fluctuations in the 10-min mean wind speed (high energy, very low cycling frequency).

This paper examines the possibility of some optimal combination of battery and ultracapacitor for energy storage in a direct current bus. The utility of the lead acid battery is that it is ubiquitously available; it has a relatively good ratio of cost to useable energy, and it is familiar for use in renewable energy and power systems applications. One of the drawbacks of lead-acid batteries is that repeated charging and discharging leads to battery failure. Due to (among other things) repeated cycling, renewable energy systems can be particularly troublesome for lead-acid battery storage [4]. Battery construction can be tailored to the application so that, for example, with thicker lead plates battery longevity may be improved in high or deep cycle applications. However, it is unfortunate that though batteries are rechargeable, using them in this manner shortens their lifespan—in some cases dramatically.

Like batteries, ultracapacitors also store electrical energy via a chemical process; however, there are several important differences between the two storage technologies. Ultracapacitors

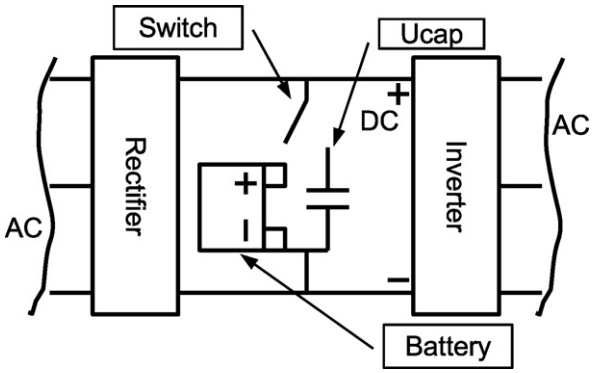

Fig. 1. Schematic of hypothetical storage integration.

are a rather new technology compared with lead-acid batteries. Manufacturers claim that cycling (in and of itself) has essentially no effect on the lifetime of ultracapacitors. Ultracapacitors can discharge at much higher rates than batteries—though only for limited durations. Yet, ultracapacitors are significantly more expensive than batteries on a cost per stored energy basis and do not possess the high volumetric energy density of lead-acid batteries. The strengths and weaknesses of the two technologies should fit well into a storage system where the ultracapacitor could compensate for frequent, short, and high power disturbances, while the battery could provide compensation for longer-term less frequent events. Fig. 1 shows a simple schematic of a hypothetical system where the storage has been inserted into a dc bus of a back-to-back type power converter.

2. Methods

The overall model has been built primarily as an extension of a simplification of an exponential decay and Miner's damage rule model described as part of the UMass battery model [5]. This double exponential decay model of has been reduced to a single exponential decay for simplicity, so now the battery life prediction equation for cycles to failure as a function of DOD uses only three coefficients:

$$C_F = a_1 + a_2 e^{a_3 \mathrm{DOD}} \quad (1)$$

Best-fit coefficients (for a_1, a_2, and a_3) for the BAE OPzS battery from [5] were obtained by minimizing the RMSE using the Quasi-Newton with BFGS Hessian update method. Table 1 shows the coefficient values obtained and 95% confidence intervals for the best-fit coefficients. Table 2 lists the datapoints used in creating the fit. Fig. 2 shows the datapoints (green crosses – DataPoints), the best curve fit obtained (blue line – BF), and also the curves using 95% confidence interval for the best-fit coefficients (red lines – 95 CI).

Table 1
Coefficient Values and 95% Confidence Intervals

Coefficient	Value	95% CI
a_1	1.405×10^3	0.870×10^3 to 1.941×10^3
a_2	1.341×10^4	0.947×10^4 to 1.735×10^4
a_3	−7.312	−9.957 to −4.675

Table 2
Data Values for Example Battery [5]

DOD	CF
0.1	8000
0.2	4000
0.3	3200
0.4	2400
0.5	1900
0.6	1600
0.7	1350
0.8	1200

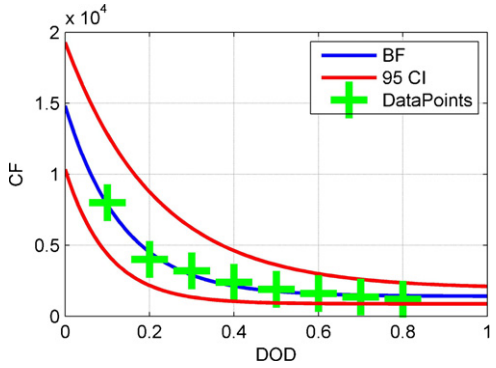

Fig. 2. Best fit RMSE to example battery.

This example battery will be used as the baseline system in the following analysis, in order to normalize the results and allow for their generalization. Therefore, DOD will be fixed at the amount for the baseline system. Fig. 3 shows a comparison of the effects of modifying the baseline system by, for example, doubling the size (thereby halving the effective DOD) or by including an Ucap as a percentage of the system total energy.

In the figure, the baseline battery system, BBS, (blue circled line) possesses a shorter cycling-life than a battery only system that is twice as large, 2 × BBS, (red circled line), a system that combines a Ucap and battery in a ratio of 0.1–0.9 of baseline energy, 1 × (0.1U + 0.9BBS), (blue crossed line), or a combination system of 0.2–1.8 of baseline energy, 2 × (0.1U + 0.9BBs), (red crossed line). Also evident in the figure is the schema for the operation of the combination system: discharges of less than the energy level of the Ucap are simply assumed to not affect

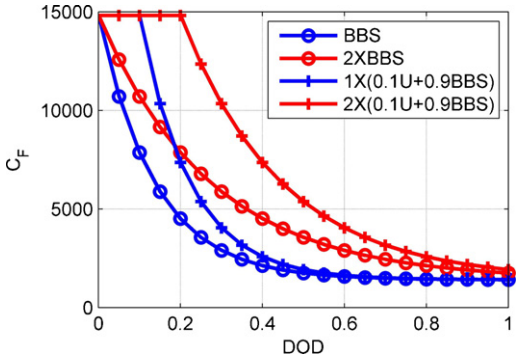

Fig. 3. Cycles to failure of systems.

the cycling-life of the combination system e.g. for DODs less than 0.1 for the 1 × (0.1U + 0.9BBS) system or for DODs less than 0.2 for the 2 × (0.1U + 0.9BBS) system.

Costs for the individual components of the model are simply taken as initial capital costs and are linear combinations of current prices of commercial deep-cycle lead-acid batteries and symmetric ultracapacitors and are approximately 5×10^{-5} US$/Joule and 1.5×10^{-2} US$/Joule, respectively [6,7]. The system costs are also normalized with respect to the baseline system. The model does not use economic methods such as net present value, though these could be readily added. As an example, the cost for the 2 × BBS system is 2 times that of the baseline, while the 1 × (0.1U + 0.9BBS) system would cost approximately 35 times the baseline system.

There are two main design variables in the system optimization: ratio of Ucap energy to system energy and overall system energy—relative to the baseline battery only system. By utilizing different energy ratios and system sizes, a wide range of cycling lifetimes and costs can be explored for the combination that minimizes the lifetime cost of the system. Both the battery and the Ucap are assumed to be ideal in the sense that only the effects of DOD on cycling life are being studied in a non-implementation specific design. This precludes over and under voltage operation, partial re-charging, and multi-cell effects. It also does not take into account any efficiencies or reduced operational abilities for either battery or Ucap. Finally, while the effect of cycling on the battery is obviously included, the Ucap is assumed to be unaffected by charge/discharge cycles.

3. Results

Before discussing the results of the system modeling, a brief discussion of the results of the curve-fit for the baseline battery system will be presented.

The curve-fit problem is solved by minimizing the root mean squared error between the candidate functions (i.e. Eq. (1) with different coefficient values) and the actual datapoints. Using a Quasi-Newton search with BFGS update method in the Matlab Optimization Toolbox [8] required 36 main loop executions and 184 function evaluations from a start of $[0\,0\,0]^T$. Using the steepest descent method to update the Hessian did not result in convergence to a solution within an acceptable number of iterations (i.e. greater than 10^4). Parallel analysis also using a least squares approach, but with Levenberg–Marquardt search utilizing the Matlab Statistics Toolbox [8] required 13 main loop executions from a start of $[0\,0\,0]^T$; resulted in the same coefficient estimates; and yielded, using the linearized estimate of the coefficient covariance, 95% confidence intervals (see Table 1) for the predicted coefficient values. Several starts from different initial conditions resulted in the same optimal final combination of coefficients, presumably this is predicted to some degree by the fact that there are eight datapoints (equally spaced over the x-axis) and only three coefficients resulting in an overconstrained problem that should have only one solution. In other words, given only three datapoints, it would be possible to fit a unique curve that would possess an RMSE of zero, since this equation has an additional five datapoints, the problem becomes

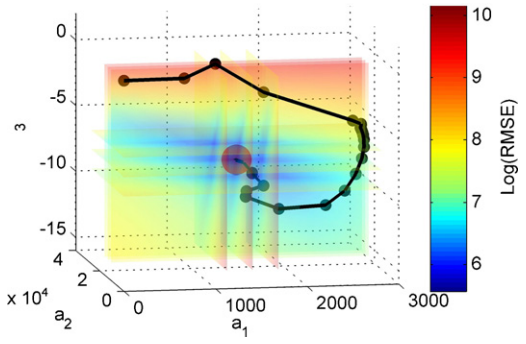

Fig. 4. Curve fit coefficients and log(RMSE).

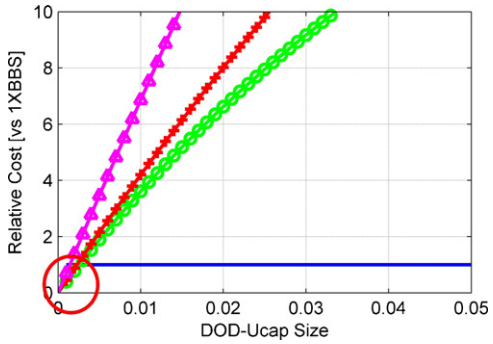

Fig. 5. Relative cost of combination system compared to life comparable battery only system: battery only system (blue Line), 10% Ucap system (green circles), 20% Ucap system (red crosses), 50% Ucap system (purple triangles).

minimizing the RMSE. The objective function to be minimized is:

$$f(a_1, a_2, a_3) = \sqrt{\frac{1}{n}\sum_{i=1}^{n}[C_{\mathrm{F},i} - (a_1 + a_2 e^{a_3 \mathrm{DOD}_i})]^2} \quad (2)$$

where i ranges from 1 to 8 (the number of datapoints). At an extremum (e.g. the minimum RMSE) the gradient of f with respect to a_1, a_2, and a_3 should vanish. In order for the extremum to be confirmed as a minimum, the Hessian of f at (at least) the extremum should be positive definite. Of course, there is no guarantee that this minimum is anything but a local minimum unless the Hessian can be demonstrated to be positive definite over the entire space of a_1, a_2, and a_3. The definition of RMSE guarantees a positive definite Hessian over the entire space for real values—due to the squared term. This means that the solution found is a global minimum for the RMSE. Fig. 4 shows a three-dimensional volume plot where the color of the region indicates the natural logarithm of the RMSE value (blue indicates smaller RMSEs while red indicates larger RMSEs). The log function has been used in the plot in order to enhance the contrast. Also shown in the figure is the optimization trajectory (the black dotted line). As expected, the trajectory points toward the smallest RMSE value.

Because the coefficients are constants, the sensitivity of the objective function (with respect to the individual datapoints) is only a function of the partial derivative with respect to each datapoint. When one differentiates the objective function, in essence, one recovers the original equation for battery life, i.e.:

$$\frac{d}{\mathrm{dDOD}_i} f = a_2 a_3 e^{a_3 \mathrm{DOD}_i} qq_i \quad (3)$$

$$\frac{d}{\mathrm{d}C_{\mathrm{F},i}} f = -qq_i C_{\mathrm{F},i} \quad (4)$$

where

$$qq_i = -C_{\mathrm{F},i} + a_1 + a_2 e^{a_3 \mathrm{DOD}_i} \quad (5)$$

Assuming that the terms common to all variables are factored out.

Because the sign of the exponent of the exponential term (i.e. a_3) is negative, the sensitivity analysis of f with respect to DOD shows that the objective function seems to more heavily weight datapoints at smaller values along the abscissa (i.e. data lying closer to the origin). Fortunately, the fitted curve in this case not only possesses a minimal RMSE, but it also seems to qualitatively fit the data very well.

Fig. 5 shows a simple comparison between the costs of a Ucap plus battery system and a battery only system that is sized to provide comparable cycle life. In order to improve legibility, the figure is normalized such that only DOD's above the Ucap ratio for each system are considered (i.e. the curve for the 10% Ucap system has been shifted by −0.1, and so on). As can be seen in the figure, as the DOD rises above the capacitor size, the relative costs of the system increase rapidly. However, there is a region (circled in red) where the capacitor/battery combination should cost less for a similar number of cycles at particular depths of discharge.

A more complicated picture emerges when the two design variables (Ucap/System energy ratio and System size) are indeed allowed to vary over the solution space. Figs. 6 and 7 illustrate the system cost over the design space, and are three-dimensional views of function values for DODs of 0.9 and 0.1 respectively; both the height along the z-axis and color spectrum indicates the function value (i.e. tall red indicates systems that cost more while low blue indicates systems that cost less).

Also visible in the figures are optimization trajectory endpoints (i.e. optimal points). As might be suspected, the non-convex nature of the solution space proves a challenge for gradient-based optimization. In the figures, one trajectory endpoint (green box) possesses a initial values that cause the search to proceed to a local minimum, while the other trajectory

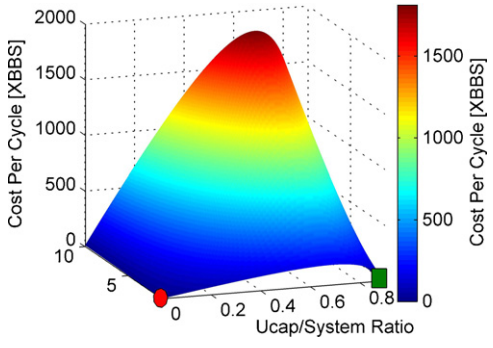

Fig. 6. System cost for 0.9 DOD.

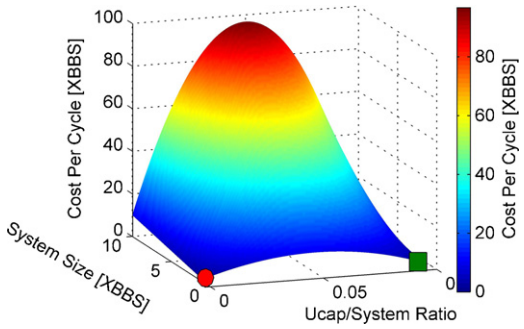

Fig. 7. System cost for 0.1 DOD.

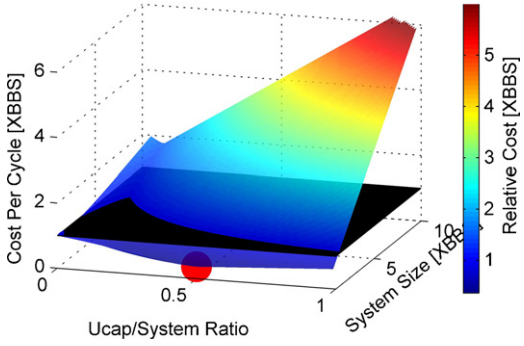

Fig. 8. Relative cost to Ucap failure, 0.5 DOD, BF coefficients.

endpoint (red circle) possesses an initial condition that causes the solution to proceed to the global optimum. The difference between the global and local optimum is that due to the nature of the model, the cost of a system that possesses a Ucap that is sized in order to match the DOD approaches zero as the number of cycles (i.e. cycle-lifetime) tends towards larger and larger values; while the baseline system cost remains at unity. This is somewhat an artifact of the model, so another analysis has been performed with an upper limit on the cycle-lifetime of the Ucap.

In this revised analysis, a lifetime limit of one million cycles has been imposed on the Ucap component, and batteries in the systems are replaced once their lifetimes have expired. In effect the question asked in this case is "How much does it cost for this system to reach one million cycles?" Figs. 8–10 present the three-dimensional results from the case where the Ucap size is allowed to vary while the DOD (again using the baseline DOD) is fixed at 0.5. In the figures the black region is the region

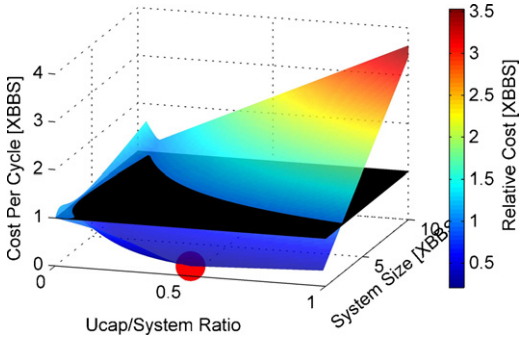

Fig. 9. Relative cost to Ucap failure, 0.5 DOD, LC coefficients.

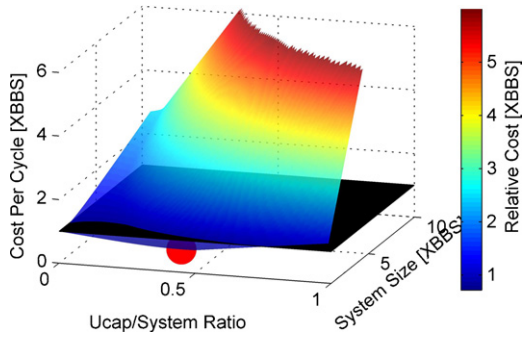

Fig. 10. Relative cost to Ucap failure, 0.5 DOD, HC coefficients.

where the cost of a combination system would be equal to a comparable battery only system; therefore systems that have costs that are below the black plane are more cost-effective than battery only systems (with exhausted battery replacement in both cases).

Fig. 8 shows results using the best-fit coefficient values – hence the caption's . . . BF Coefficients'. Figs. 9 and 10 use coefficient values from the confidence interval limits. Fig. 9 shows that the region of cost-effectiveness for a Ucap/battery system has grown (as expected) due to the use of the confidence interval coefficients that result in a reduced cycling capability for the battery portion of the system – the LC (low cycle) coefficients. Fig. 10 also shows expected results in that the region of cost-effectiveness has shrunk due to the use of the confidence interval coefficients that result in increased cycling capability for the battery portion of the system – the HC (high cycle) coefficients. Even using the HC coefficients, there is still a region where the Ucap/battery system should be more cost-effective than a strictly battery-based system.

Neither the minimums (with Ucap to system ratio = 0.5 and system size = 1) nor the fact that a gradient-based optimization algorithm works well (for the convex solution space) is surprising. The figures are representative of the findings for all other DODs.

What is more surprising, however, are the results presented in Figs. 11–14 . In this analysis, the Ucap to system energy is fixed at given values (in the case of Figs. 11 and 12 Ucap/System energy ratio = 0.1) and the DOD is allowed to vary. Figs. 13 and 14 show the results of a similar analysis for energy ratio = 0.5. The analysis has been performed using the

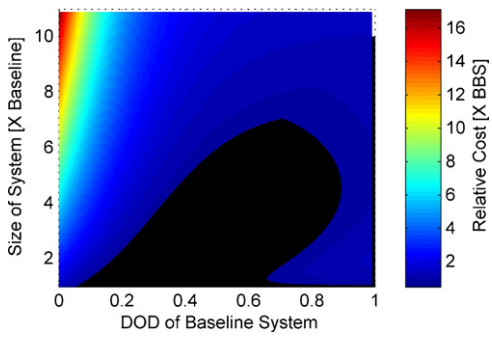

Fig. 11. Relative cost to Ucap failure, 0.1 Ucap energy ratio, BF coefficients.

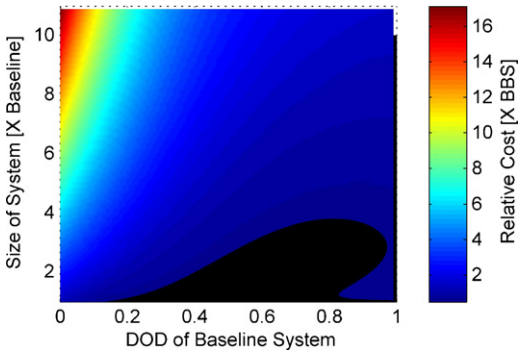

Fig. 12. Relative cost to Ucap failure, 0.1 Ucap energy ratio, HC coefficients.

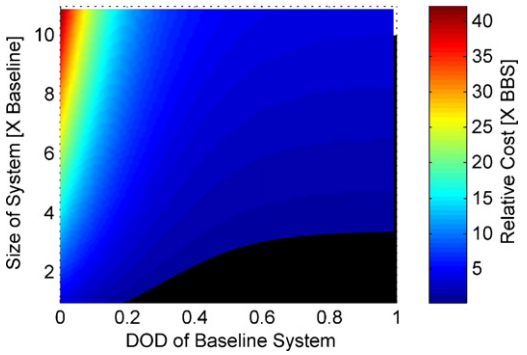

Fig. 13. Relative cost to Ucap failure, 0.5 Ucap energy ratio, BF coefficients.

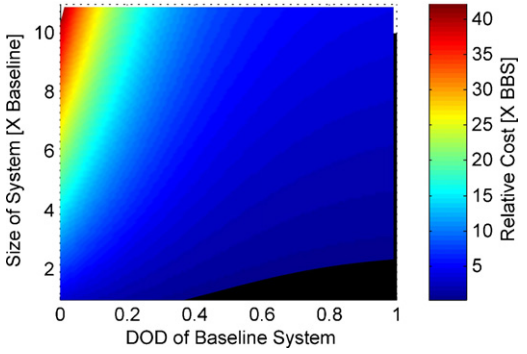

Fig. 14. Relative cost to Ucap failure, 0.5 Ucap energy ratio, HC coefficients.

best-fit coefficients (Figs 11 and 13) and the more limiting (in terms of cost-effectiveness) HC coefficients (Figs 12 and 14).

As can be seen in each of the figures, there is a region (in black) where the cost of a relatively small amount of Ucap storage can offset the cost of the batteries required (and therefore provide a lower overall system cost) over a wide range of DODs. This region changes shape (though seems to remain convex) as the Ucap to system energy ratio changes.

4. Discussion

Ultracapacitor cost is projected to decrease [7] and the effect of cost reductions will be to increase the size of the region of the below baseline system cost. Fig. 15 shows the results of the high-cycle system cost analysis using the projected cost of ultracapacitors in a system identical to that used for Fig. 13;

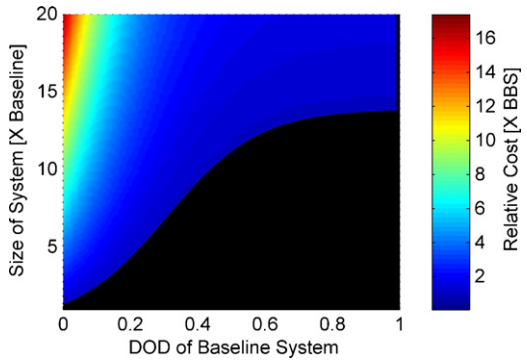

Fig. 15. Relative cost to Ucap failure, 0.5 Ucap energy ratio, projected Ucap cost, BF coefficients.

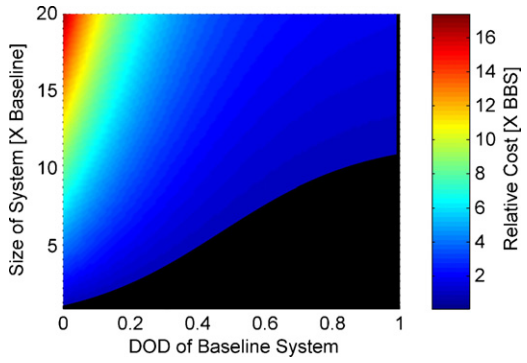

Fig. 16. Relative cost to Ucap failure, 0.5 Ucap energy ratio, projected Ucap cost, HC coefficients.

the systems used in the analysis for Figs. 14 and 16 are also identical.

When Figs. 15 and 16 is compared with Figs. 13 and 14, it can be seen that the area of applicability has significantly increased. It is not immediately visible in the figures that the overall system cost compared to the results shown in Figs. 13 and 14 (i.e. the values on the z-axis) has also decreased substantially.

5. Conclusion

The results of the fixed Ucap-to-system energy-ratio with varying depths of discharge are very encouraging, in that they imply that a small amount of Ucap storage may reduce overall system lifetime cost (to a large number of cycles) over a wide range of depths of discharge. This ability to benefit a range of DODs will be important in applications where the DOD can vary significantly, for example short-term renewable power smoothing.

High cycling applications are present in many areas of the electrical power system. The utility of this simple model is to show that a small amount of Ucap storage may well reduce battery-based smoothing system overall lifetime cost. This provides the motivation to investigate further including such issues as more sophisticated modeling (for each component, the system as a whole, and the loading conditions to which such a system will be subject) and methods of implementation of such a hybrid storage system.

References

[1] F.C. Kaminsky, R.H. Kirchoff, C.Y. Syu, J.F. Manwell, J. Sol. Energy Eng. 113 (1991) 280–289.
[2] T. Heggem, R. Lende, J. Løvseth, J. Atmos. Sci. 55 (1998) 2907–2917.
[3] J. Apt, J. Power Sources 169 (2007) 369–374.
[4] A.J. Ruddell, A.G. Dutton, H. Wenzl, C. Ropeter, D.U. Sauer, J. Merten, C. Orfanogsannis, J.W. Twidell, P. Vezin, J. Power Sources 112 (2002) 531–546.
[5] H. Binder, T. Cronin, P. Lundsager, J.F. Manwell, U. Abdulwahid, I. Baring-Gould, RisøNational Laboratory Report, Risø-R-1515(EN), 2005.
[6] Northern Arizona Wind & Sun, "Deep Cycle Batteries" http://store.solar-electric.com/suprdecyba.html. Last Accessed 05/21/07.
[7] A. Burke, Proceedings of the IEEE Conference on Vehicle Power and Propulsion, Chicago Illinois, 2005, pp. 356–366.
[8] The Mathworks Inc., Natick, MA.